Supplementary Information

A Strongly Greenish-blue-emitting Cu₄Cl₄ Cluster with Efficient Spin-Orbit Coupling (SOC): Fast Phosphorescence versus Thermally Activated Delayed Fluorescence

Xu-Lin Chen,[a] Rongmin Yu,[a] Xiao-Yuan Wu[a], Dong Liang[a, b], Ji-Hui Jia[a], and Can-Zhong Lu*[a]

[a.] Key Laboratory of Design and Assembly of Functional Nanostructures, Fujian Institute of Research on the Structure of Matter, Chinese

Academy of Sciences, Fuzhou, Fujian, 350002, P. R. China. E-mail: czlu@fjirsm.ac.cn.

[b.] Graduate University of Chinese Academy of Sciences, Beijing, 100049, China.

23rd May 2016

Note added after first publication: This Supplementary Information file replaces that originally published on 18th April 2016, and includes a citation to work by M. J. Leitl *et al.* as ref. 9.

General

All reactions were performed under nitrogen atmosphere using standard Schlenk techniques unless specified. All starting materials were purchased from commercial sources and used as received. Solvents were freshly distilled over appropriate drying reagents. ¹HNMR spectrum of the ligand was recorded on a Bruker Avance III 400MHz NMR spectrometer. Elemental analyses (C, H, N) was carried out with an Elementar Vario EL III elemental analyzer. Photoluminescence spectra were recorded on a HORIBA Jobin-Yvon FluoroMax-4 spectrometer. Lifetime measurements were performed by multi-channel scaling (MCS) mode on the same fluorimeter equipped with a spectraLED pulsed source (373 nm). Signals were collected using a FluoroHub module and analyse by the DAS6 Decay Analysis software (HORIBA Jobin-Yvon). The variable-temperature measurements were carried out on corresponding instruments by using the additional LINKAM THMS600 system with a variable-temperature range of 77 K-873 K. The photoluminescence quantum yields were defined as the number of photons emitted per photon absorbed by the systems and measured by FluoroMax-4 equipped with an integrating sphere. The measurements and the characterizations of the Cu(I) complex in solutions are difficult to be performed for its poor solubility.

X-ray Crystallographic Analysis

Diffraction data of the Cu(I) complex was collected on a SuperNova, Atlas diffractometer equipped with graphite-monochromated Mo Kα radiation (λ = 0.71073 Å). Structure was solved by direct method and refined by full-matrix least-squares method with SHELXL-97 program package. Hydrogen atoms were added in idealized positions. All nonhydrogen atoms were refined anisotropically. Details of crystal and structure refinement are listed in **Table S1**. Selected bond length and bond angles are listed in **Table S2**. CCDC 1446745 contains the supplementary crystallographic data for the complex.
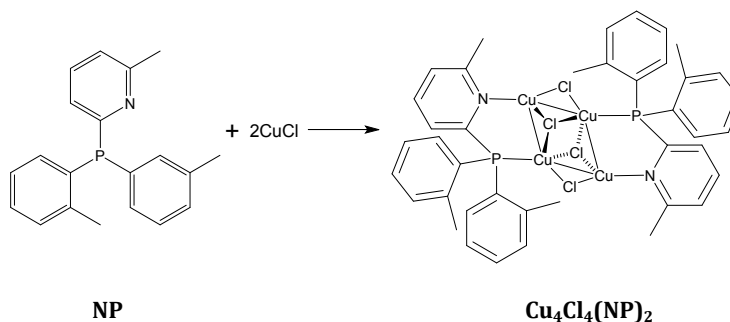
Synthesis of the ligand: 2-(di-o-tolylphosphino)-6-methylpyridine (NP)

NP
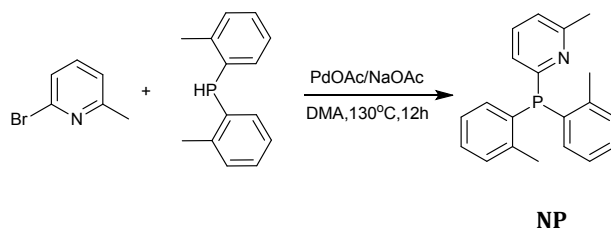
The suspension of 0.86 g (5.0 mmol) 2-bromo-6-methylpyridine, 0.82 g (10.0 mmol) NaOAc and 2.5 mg (0.01 mmol) Pd(OAc), in 10 ml DMA was charged with 1.07 g (5 mmol) di-o-tolylphosphine and heated at 130°C for 12 h. The reaction mixture was poured into 100 ml of water and the precipitate formed was collected by filtration. The crude product was purified by column chromatography on silica gel to afford a white solid (1.2g, 79%). ^{1}HNMR (400 MHz, DMSO) δ 7.62 (dd, J = 7.6, 6.0 Hz, 1H), 7.37-7.28 (m, 4H), 7.21 (d, J = 7.8 Hz, 1H), 7.19-7.10 (m, 2H), 6.71-6.58 (m, 3H), 2.47 (s, 3H), 2.35 (s, 6H). The NMR spectrum of this ligand:

400 MHz, DMSO
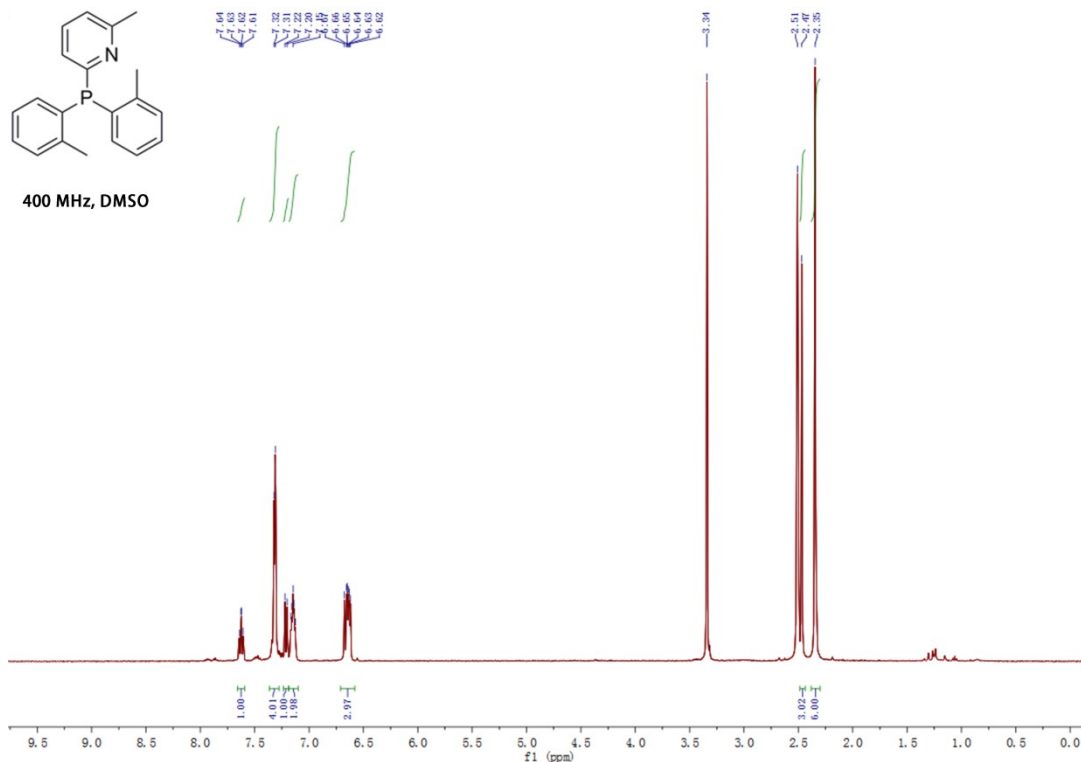
Synthesis of cuprous complex: $Cu_4Cl_4(NP)_2$

NP   **$Cu_4Cl_4(NP)_2$**

The suspension of CuCl (1 mmol, 0.099 g) and 2-(di-o-tolylphosphino)-6-methylpyridine (NP) (0.5 mmol, 0.153 g)

in 6 ml CH_2Cl_2 was stirred at room temperature for 3 hours. Colourless single crystal of the cuprous complex suitable for X-ray diffraction measurement was obtained by slow diffusion of ether into the CH_2Cl_2 solution of the product. Yield: 0.16 g (63%). Anal. calcd for $C_{40}H_{40}Cl_4Cu_4N_2P_2$: C, 47.72; H, 4.00; N, 2.78. Found: C, 47.55; H, 3.94; N, 2.71.

Computational methodology

The density functional theory (DFT) and time-dependent DFT (TD-DFT) calculations were performed with the Gaussian 09 program package,[1] using the hybrid Becke three-parameter Lee-Yang-Parr (B3LYP) functional level.[2,3] The input structures were extracted from the X-ray crystallographic data. In all calculations, the relativistic effective core potential (RECP) and the associated basis sets Lanl08 (f) and Lanl08 (d),[4] which are the revised version of original Hay-Wadt basis set, were employed for the Cu(I) atoms. All-electron basis set of 6-31G* was used for other non-metal atoms of Cl, P, N, C and H. Visualization of the optimized structures and frontier molecular orbitals were performed by GaussView. The partition orbital composition was analyzed by using the Multiwfn 2.4 program.[5]

Deduction and explanation for equation 1

For a system of thermally equilibrated excited states (three T_1 substates I, II, III and singlet state S_1), the temperature-dependent averaged decay time τ is given by the following expression: [6,7]

$$\tau = \frac{1 + \exp\left(-\frac{\Delta E_{II-I}}{k_B T}\right) + \exp\left(-\frac{\Delta E_{III-I}}{k_B T}\right) + \exp\left(-\frac{\Delta E_{ST}}{k_B T}\right)}{\frac{1}{\tau_I} + \frac{1}{\tau_{II}}\exp\left(-\frac{\Delta E_{II-I}}{k_B T}\right) + \frac{1}{\tau_{III}}\exp\left(-\frac{\Delta E_{III-I}}{k_B T}\right) + \frac{1}{\tau(S_1)}\exp\left(-\frac{\Delta E_{ST}}{k_B T}\right)}$$

eqn S1

The energy gap between the S_1 and T_1 states (ΔE_{ST}) is determined to be about 0.08 eV (645 cm^{-1}). Although it is very small, we cannot treat the S_1 and T_1 as degenerate states when compared with the splitting of the T_1 state, that is, the zero-field splitting (ZFS). For Cu(I) complexes, with the spin orbit coupling (SOC) constant of copper being about five times smaller than that of iridium or platinum, $\Delta E(ZFS)$ values of the order of 1 to 10 cm^{-1} are expected, which is significantly smaller than ΔE_{ST}.[8] Considering the energetic quasi-degeneracy of the three T_1 substates, the average decay time of T_1 is

$$\tau(T_1) = \frac{1}{3\left(\frac{1}{\tau_I} + \frac{1}{\tau_{II}} + \frac{1}{\tau_{III}}\right)}$$

eqn S2

Then, the **eqn S1** simplifies to **eqn 1**

$$\tau = \frac{1 + \frac{1}{3}\exp\left(-\frac{\Delta E_{ST}}{k_B T}\right)}{\frac{1}{\tau(T_1)} + \frac{1}{3\tau(S_1)}\exp\left(-\frac{\Delta E_{ST}}{k_B T}\right)}$$

Relative contributions of TADF and phosphorescence

In order to evaluate the relative contributions of TADF and phosphorescence, we estimate the percentage of the intensity originating from the singlet $I(S_1)$ and from the triplet state $I(T_1)$ relative to the total intensity I_{tot} in dependence of the temperature.[9] The intensity is proportional to the population of the individual state N and to the corresponding radiative rate constant k_r, so we can obtain

$$I(S_1) = \alpha N(S_1)k_r(S_1) = \alpha N(S_1)\Phi_{PL}(S_1)\tau(S_1)^{-1}$$

eqn S3

$$I(T_1) = \alpha N(T_1)k_r(T_1) = \alpha N(T_1)\Phi_{PL}(T_1)\tau(T_1)^{-1}$$

eqn S4

Herein, α is the proportionality constant that is same in both the equations. For rough estimates, we assume that the quantum yields $\Phi_{PL}(S_1)$ and $\Phi_{PL}(T_1)$ do not depend on the temperature, and we use the Φ_{PL} values determined at 293 K and 77 K, respectively (**Table 1**). Assuming that the populations of both states follow a Boltzmann distribution (fast equilibration), the relative intensities can be expressed as follows

$$\frac{I(T_1)}{I_{tot}} = \frac{I(T_1)}{I(S_1) + I(T_1)} = \left[1 + \frac{I(S_1)}{I(T_1)}\right]^{-1} = \left[1 + \frac{\alpha N(S_1)\Phi_{PL}(S_1)\tau(S_1)^{-1}}{\alpha N(T_1)\Phi_{PL}(T_1)\tau(T_1)^{-1}}\right]^{-1} =$$

$$\left[1 + \frac{N(S_1)\Phi_{PL}(S_1)\tau(T_1)}{N(T_1)\Phi_{PL}(T_1)\tau(S_1)}\right]^{-1}$$

$$= \left[1 + \frac{\Phi_{PL}(S_1)\tau(T_1)g(S_1)}{\Phi_{PL}(T_1)\tau(S_1)g(T_1)}\exp\left(-\frac{\Delta E_{ST}}{k_B T}\right)\right]^{-1}$$

eqn S5

$$\frac{I(S_1)}{I_{tot}} = 1 - \frac{I(T_1)}{I_{tot}} = 1 - \left[1 + \frac{\Phi_{PL}(S_1)\tau(T_1)g(S_1)}{\Phi_{PL}(T_1)\tau(S_1)g(T_1)}\exp\left(-\frac{\Delta E_{ST}}{k_B T}\right)\right]^{-1}$$

eqn S6

where $g(S_1) = 1$ and $g(T_1) = 3$ are the degeneracy factors for the singlet and the triplet states, respectively. The splitting of the T_1 state, that is, the zero-field splitting (ZFS), is distinct in organo-transition-metal compounds due to the high metal participation and large spin-orbit coupling. So, we take into account the degeneracy factors for the singlet and the triplet states ($g(S_1) = 1$ and $g(T_1) = 3$) in evaluating the populations of the two states (Boltzmann distribution).

The plots shown in **Fig. 2c** can be obtained using **eqn S5** and **eqn S6**, in which the parameters have been determined by **eqn 1** (see **Fig. 2b**). As a result, the relative contributions of TADF and phosphorescence are depicted visually in **Fig. 2c**.

The overall emission decay time τ (293 K) versus the decay time of the lowest triplet state τ (T$_1$)

The simulation result (**Fig. 2d**) of the overall emission decay time $\tau(293\ K)$ versus the decay time of the lowest triplet state $\tau(T_1)$ can be obtained approximately according to the following equation:

$$\tau(293\ K) = \frac{1 + \dfrac{1}{3}\exp\left(-\dfrac{\Delta E_{ST}}{k_B T}\right)}{\dfrac{1}{\tau(T_1)} + \dfrac{1}{3\tau(S_1)}\exp\left(-\dfrac{\Delta E_{ST}}{k_B T}\right)}$$

eqn S7

Table S1. Crystal data and structure refinement for the cuprous complex $Cu_4Cl_4(NP)_2$.

Complex	$Cu_4Cl_4(NP)_2$
Empirical formula	$C_{40}H_{40}Cl_4Cu_4N_2P_2$
Formula weight	1006.64
Crystal system	monoclinic
Space group	P2(1)/c
a (Å)	11.1272(3)
b (Å)	13.5250(4)
c (Å)	13.4866(4)
α (deg)	90.00
β (deg)	104.147(3)
γ (deg)	90.00
V (Å^3)	1968.11(10)
Z	2
ρ_{calc} (g cm^{-3})	1.699
μ (mm^{-1})	2.518
F(000)	1016
λ (Å)	0.71073
Reflections collected/unique	3922/3366
Θ range (deg)	1.89-26.40
GOF on F^2	1.078
R_1/wR_2 [I ≥ 2σ(I)]	0.0451/0.1291
R_1/wR_2 (all data)	0.0525/0.1369

Table S2. Selected bond length (Å) and bond angles (deg) for the cuprous complex $Cu_4Cl_4(NP)_2$.
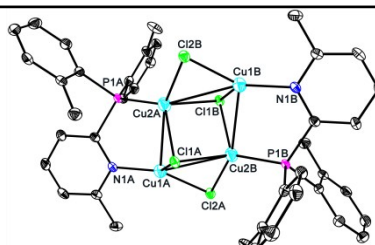
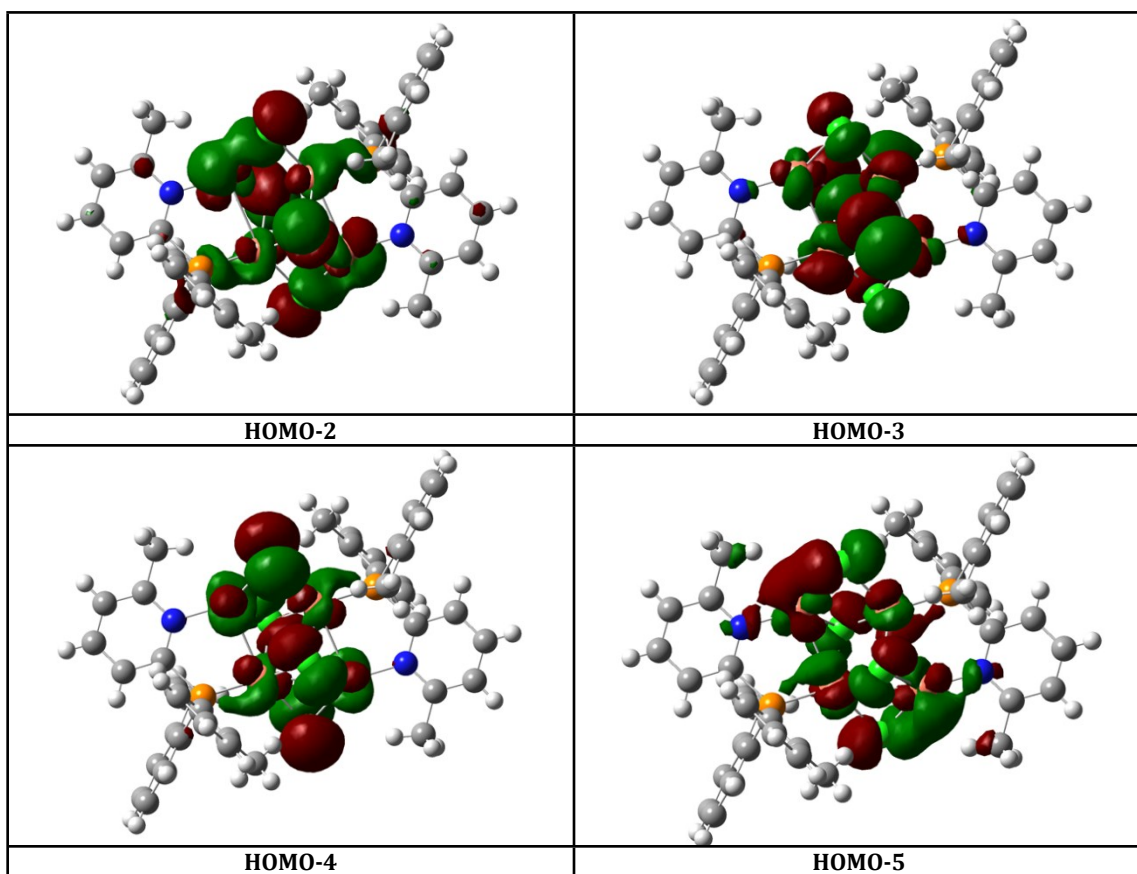|	
Cu1A-Cu2A	2.7827(7)
Cu1A-Cu2B	2.9202(7)
Cu1A-N1A	1.9687(3)
Cu2A-P1A	2.1955(10)
Cl1A-Cu1A	2.4115(10)

Cl1A-Cu2A	2.3796(9)
Cl1A-Cu2B	2.4791(9)
Cl2A-Cu1A	2.2528(10)
Cl2A-Cu2B	2.3778(9)
Cu2A-Cu1A-Cu2B	65.79(2)
N1A-C-P1A	118.335(3)

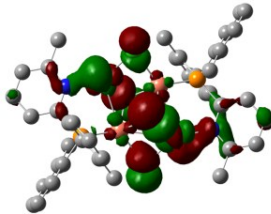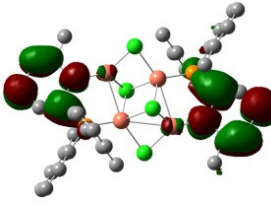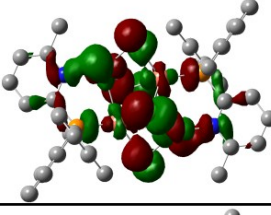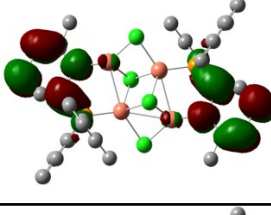**Table S3** The frontier orbitals from HOMO-5 to LUMO+1 of $Cu_4Cl_4(NP)_2$ in the X-ray structure.

LUMO+1	**LUMO**

HOMO	**HOMO-1**

HOMO-2

HOMO-3

HOMO-4

HOMO-5
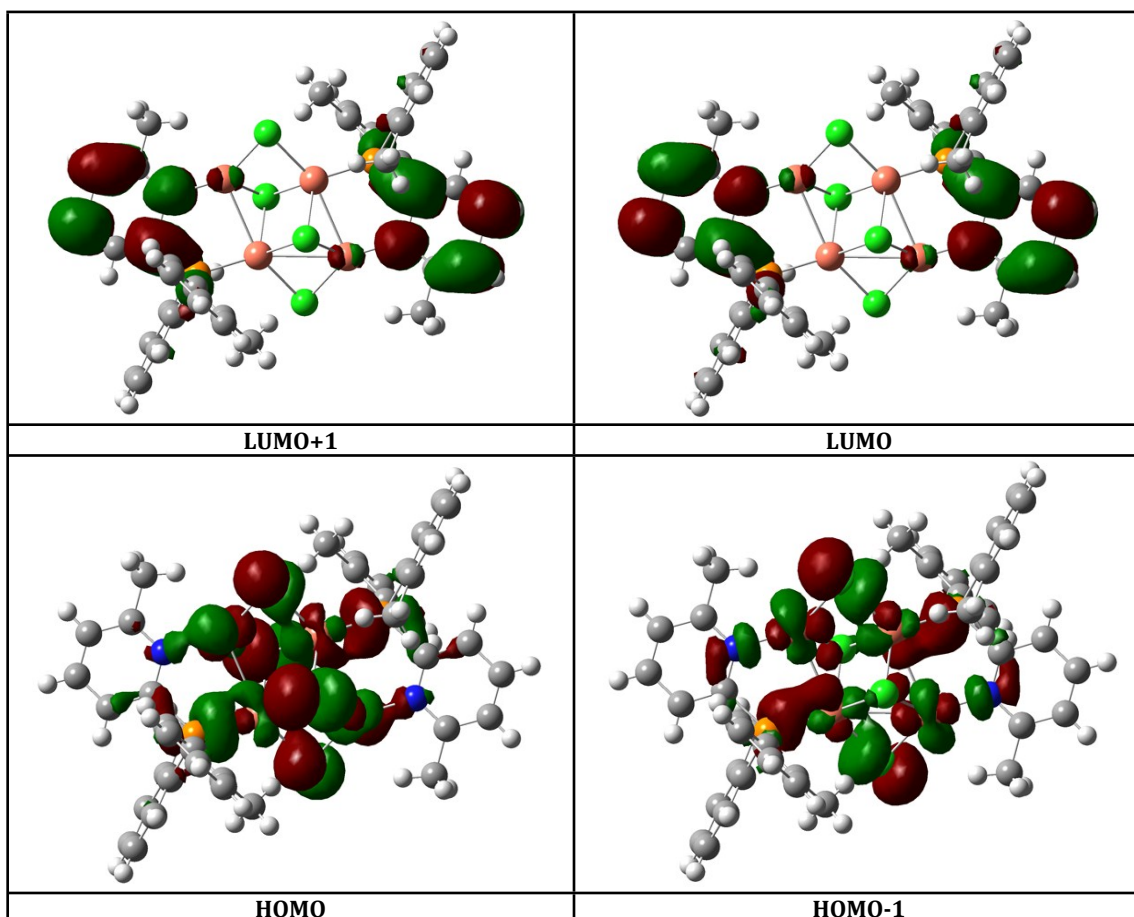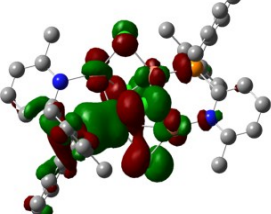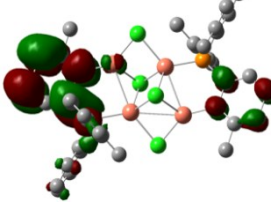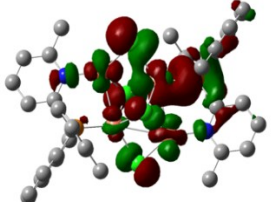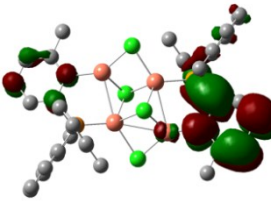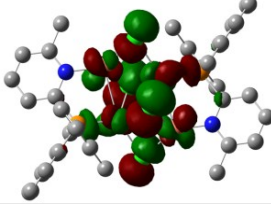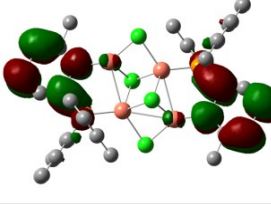
Table S4 Composition of the frontier orbitals of $Cu_4Cl_4(NP)_2$ in the optimized X-ray structure.

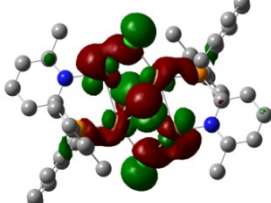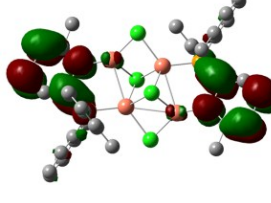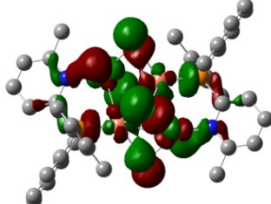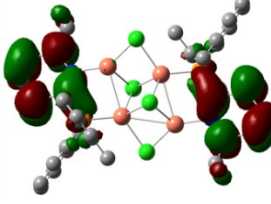|		E(eV)	Cu	Cl	Ligand
$Cu_4Cl_4(NP)_2$	HOMO-11	-6.313	82.760955%	10.620938%	6.61811%
	HOMO-10	-5.987	60.364991%	34.439808%	5.1952%
	HOMO-9	-5.959	65.696562%	26.471260%	7.83218%
	HOMO-8	-5.932	59.531832%	21.529596%	18.93857%
	HOMO-7	-5.823	75.322902%	11.760536%	12.91656%
	HOMO-6	-5.742	75.949770%	18.091198%	5.95903%
	HOMO-5	-5.633	53.687561%	42.384144%	3.92829%
	HOMO-4	-5.578	57.937114%	38.646679%	3.41621%
	HOMO-3	-5.252	60.411307%	29.927243%	9.66145%
	HOMO-2	-5.137	54.346852%	35.598538%	10.05461%
	HOMO-1	-5.116	65.578312%	17.474712%	16.94698%
	HOMO	-5.061	53.186365%	31.046745%	15.76689%
	LUMO	-1.546	3.541482%	0.894050%	95.56447%
	LUMO+1	-1.529	6.464548%	0.797420%	92.73803%
	LUMO+2	-1.034	7.557117%	0.234632%	92.20815%

Table S5 Low energy vertical transitions, with their corresponding oscillator strengths (f), natural transition orbitals, and assignments for the studied complex calculated for the X-ray geometry.

State	E(nm)	f	Main contribution	Hole	Electron
T_1	465.77	0	HOMO→LUMO (42%)		
S_1	439.28	0.0174	HOMO-1 →LUMO (41%)		
S_3	423.39	0.0001	HOMO-1 →LUMO (47%)		

S_4	423.32	0.0244	HOMO-2 →LUMO (81%)		
S_6	413.25	0.029	HOMO-2 →LUMO+1 (86%)		
S_7	389.13	0.0132	HOMO-3 →LUMO (77%)		
S_{10}	367.11	0.0036	HOMO→ LUMO+3 (61%)		

Table S6 Compositions of hole and electron in the S_1 and T_1 of $Cu_4Cl_4(NP)_2$ based on the X-ray structure.

		Cu	Cl	ligand
S_1	hole	61.4%	26.2%	12.4%
	electron	5.4%	0.9%	93.7%
	difference	56.0%	25.3%	-81.4%
T_1	hole	62.6%	28.5%	8.9%
	electron	4.9%	1.2%	93.9%
	difference	57.7%	27.3%	-85.0%

References

1   G. W. T. M. J. Frisch, H. B. Schlegel, G. E. Scuseria, M. A. Robb, J. R. Cheeseman, G. Scalmani, V. Barone, B. Mennucci, G. A. Petersson, H. Nakatsuji, M. Caricato, X. Li, H. P. Hratchian, A. F. Izmaylov, J. Bloino, G. Zheng, J. L. Sonnenberg, M. Hada, M. Ehara, K. Toyota, R. Fukuda, J. Hasegawa, M. Ishida, T. Nakajima, Y. Honda, O. Kitao, H. Nakai, T. Vreven, J. A. Montgomery Jr., J. E. Peralta, F. Ogliaro, M. Bearpark, J. J. Heyd, E. Brothers, K. N. Kudin, V. N. Staroverov, R. Kobayashi, J. Normand, K. Raghavachari, A. Rendell, J. C. Burant, S. S. Iyengar, J. Tomasi, M. Cossi, N. Rega, J. M. Millam, M. Klene, J. E. Knox, J. B. Cross, V. Bakken, C. Adamo, J. Jaramillo, R. Gomperts, R. E. Stratmann, O. Yazyev, A. J. Austin, R. Cammi, C. Pomelli, J. W. Ochterski, R. L. Martin, K. Morokuma, V. G. Zakrzewski, G. A. Voth, P. Salvador, J. J. Dannenberg, S. Dapprich, A. D. Daniels,

Ö. Farkas, J. B. Foresman, J. V. Ortiz, J. Cioslowski and D. J. Fox, Gaussian 09, Revision D.01, Gaussian, Inc., Wallingford, CT, 2009.

2   C. Lee, W. Yang and R. G. Parr, *Phys. Rev. B: Condens. Matter*, 1988, **37**, 785.

3   A. D. Becke, *J. Chem. Phys.*, 1993, **98**, 5648.

4   L. E. Roy, P. J. Hay and R. L. Martin, *J. Chem. Theor. Comput.*, 2008, **4**, 1029.

5   T. C. Lu and F. W. Chen, *J. Comput. Chem.*, 2012, **33**, 580.

6   M. J. Leitl, V. A. Krylova, P. I. Djurovich, M. E. Thompson and H. Yersin, *J. Am. Chem. Soc.*, 2014, **136**, 16032.

7   H. Yersin, A. F. Rausch and R. Czerwieniec, *Physics of Organic Semiconductors*, Wiley-VCH Verlag, New York, 2012, 371.

8   H. Yersin, A. F. Rausch, R. Czerwieniec, T. Hofbeck, T. Fischer, *Coord. Chem. Rev.* 2011, **255**, 2622.

9   M. J. Leitl, F. R. Kuchle, H. A. Mayer, L. Wesemann and H. Yersin, *J. Phys. Chem. A*, 2013, **117**, 11823.